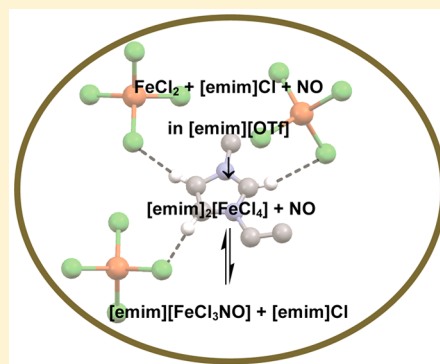


Studies on the Reaction of Iron(II) with NO in a Noncoordinating Ionic Liquid

Svetlana Begel,[†] Ralph Puchta,[†] Jörg Sutter,[†] Frank W. Heinemann,[†] Lutz Dahlenburg,[†] and Rudi van Eldik^{*,†,‡}[†]Department of Chemistry and Pharmacy, University of Erlangen-Nürnberg, Egerlandstr. 1, 91058 Erlangen, Germany[‡]Faculty of Chemistry, Jagiellonian University, Ingardena 3, 30-060 Krakow, Poland

ABSTRACT: In an earlier study we investigated the reaction of iron(II) chloride with NO in a strongly coordinating ionic liquid 1-ethyl-3-methylimidazolium dicyanamide [emim][dca] and showed that the actual reactive species in solution was $[\text{Fe}^{\text{II}}(\text{dca})_2\text{Cl}]^+$. For the present report we investigated in detail how this reaction could proceed in a noncoordinating ionic liquid 1-ethyl-3-methylimidazolium trifluoromethylsulfonate [emim][OTf]. The donor ability of OTf^- is much lower than that of dca^- , such that the solubility of FeCl_2 in [emim][OTf] strongly depended on other donors like water or chloride ions present or added to the ionic liquid. On increasing the chloride concentration in [emim][OTf], the tetrachloridoferrate complex $[\text{emim}]_2[\text{FeCl}_4]$ was formed, as verified by X-ray crystallography. This complex undergoes reversible binding of NO, for which the UV-vis spectral characteristics of the green-brown nitrosyl product resembled that found for the corresponding nitrosyl complexes formed in water and [emim][dca] as solvents. A detailed analysis of the spectra revealed that the $\{\text{Fe}-\text{NO}\}^7$ species has $\text{Fe}^{\text{II}}-\text{NO}^{\bullet}$ character in contrast to $\text{Fe}^{\text{III}}-\text{NO}^-$ as found for the other solvents. The formation constant, however, is much higher than in [emim][dca], lying closer to the value found for water as solvent. Surprisingly, the Mössbauer spectrum found in [emim][OTf] is very unusual and unsimilar to that found in water and [emim][dca] as solvents, pointing at a different electron density distribution between Fe and NO in $\{\text{Fe}-\text{NO}\}^7$. First, the high isomer shift points to the presence of iron(II) species in solution, thus indicating that upon NO binding no oxidation to iron(III) occurs. Second, the negligible quadrupole splitting suggests a high local symmetry around the iron center. The nitrosyl product is suggested to be $[\text{Fe}^{\text{II}}\text{Cl}_3\text{NO}]^-$, which is supported by electron paramagnetic resonance (EPR) and IR measurements. The nature of the Fe(II) complexes formed in [emim][OTf] depends on the additives required to dissolve FeCl_2 in this ionic liquid.



INTRODUCTION

Most chemical reactions performed in a laboratory or in industry take place in solution. In synthesis, chromatographic separation, extraction, purification, analysis and spectroscopy, and crystal growth and cleaning, the required solvent can also be a reactant.¹ Therefore, the solvent can play a very important role in solution chemistry.² Furthermore, many important chemical reactions are performed in organic solvents, but their use is often problematic owing to toxicity, volatility, flammability, and environmental hazards.³ The development of alternative solvent strategies that would allow efficient recovery and reuse of the solvent is of great importance if environmental damage is to be avoided.⁴

Ionic liquids (ILs), low-melting molten salts composed entirely of ions, are a relatively recent class of liquids attracting increasing interest as greener alternatives to conventional organic solvents with the aim of facilitating sustainable chemistry.⁵ Because of their unusual physical and chemical properties,⁶ such as high thermal stability,⁷ lack of inflammability,⁸ low volatility,⁹ chemical stability,¹⁰ and excellent solubility of many organic compounds,¹¹ many potential applications, such as synthesis,¹² (bio)catalysis,¹³ separation

processes,¹⁴ material science,¹⁵ and development of new electrical and electrochemical devices,¹⁶ continue to expand significantly.

The application of ionic liquids as substitutes for common molecular solvents is limited by the dual influence they can have in terms of both positive and negative impacts on chemical reactions. It is known from the literature that some reactions are improved on transferring them to an ionic liquid medium in terms of the outcome, selectivity, or reaction rate, whereas others are decelerated or even completely prevented.¹⁷ The reason for these effects is not always clear, but it is expected that the ionic components of the ionic liquid can interact with reactants, products, or catalyst. Interaction with the catalyst or activated species of metal complexes could lead to a change in reaction rate or even selectivity based on structural modifications. In addition, interactions with reactants or products by solvation or ion-pair formation can influence the processes by changing the activation barriers or the nucleophilicity of substrates. The search for the origin of a

Received: March 16, 2015

Published: July 8, 2015

certain effect is often complicated by various interactions, such that information on the outcome or rate of a reaction is not sufficient to draw definite conclusions. A real understanding of the occurrences during the reaction and thus the possibility to control the process are best achieved by a detailed mechanistic investigation.

Numerous publications from our group demonstrated that ionic liquids in general can be considered as normal solvents and a wide range of experimental techniques can be applied to study their behavior.^{18–20} However, the same investigations revealed a distinct influence of ionic liquids as reaction medium on the chemical processes carried out in them, often analogous to the influence known from conventional solvents.²¹ Recent work from our group has focused on the behavior of transition metal compounds during well-known fundamental reactions in different ILs.^{18,19,22,23} We found a significant influence of the applied ILs on the different steps of the reactions: from altering the nature of the starting compounds, including formation of ion pairs or even of a completely new species due to the noteworthy nucleophilicity of the IL's anions, to mechanistic modifications resulting in the deviation of reaction rates from the conventional values. We concluded that ionic liquids are anything but innocent solvents, especially those containing anions that are clearly able to coordinate to metal centers.

In the framework of our interest in the potential influence of ILs as reaction media on transition metal species, we extended our investigations to an ionic liquid with a likely non-coordinating anion to study the interference of a wider variety of solvents. We present here our first results on the reaction of FeCl_2 with NO in 1-ethyl-3-methylimidazolium trifluoromethylsulfonate, $[\text{emim}][\text{OTf}]$, as solvent. The structure and physical properties of this IL are given in an earlier paper from our group.¹⁸

The selected IL is among the best studied to date and is readily available. Since it was previously found that even a very low concentration of a synthetic impurity can dramatically affect the underlying reaction mechanism,²⁰ the purity of the applied $[\text{emim}][\text{OTf}]$ was thoroughly checked, including the exact determination of water and chloride content. The latter two components are significantly better nucleophiles than triflate, and their presence in the IL at high concentrations, compared to the applied amount of metal species, could affect the experimental results, simulating the relevant nucleophilicity of the ionic liquid itself. Furthermore, we applied various spectroscopic measurements, like UV–vis, IR, and Mössbauer, to improve our understanding of the occurrences in the studied IL.

EXPERIMENTAL SECTION

Materials. All chemicals used were of analytical reagent grade and of the highest purity commercially available. The water used was double-distilled and deionized. FeCl_2 anhydrous, purchased from Sigma-Aldrich, was used as a source for the Fe(II) solutions. NO gas (Praxair Deutschland GmbH & Co. KG, Bopfinger, purity 3.0) was cleaned from trace amounts of higher nitrogen oxides by passing it through concentrated KOH solution, an Ascarite II column (NaOH on silica gel, Sigma-Aldrich), and a phosphorus pentoxide column. If not stated otherwise, all experiments were performed under an inert gas atmosphere.

Preparation of the Ionic Liquids. The purchased materials were worked up to obtain the optical purity required for the applied spectroscopic investigations. $[\text{emim}][\text{OTf}]$ was obtained from Io-Li-Tec GmbH & Co. KG and purified before use by repeated recrystallization (liquid/methanol 1:1) and stirring with activated

charcoal (Norit A Supra) for 3–4 days. Afterward it was dried under vacuum at 60 °C for 3–4 days and finally stored over molecular sieves (type 3 A, nominal pore size 3 Å, obtained from Fisher Chemicals). The water and chloride content for every new batch were determined by Karl Fischer titration and ion chromatography, respectively. The chloride concentration of the ionic liquid used for EPR measurements and the determination of the equilibrium constant in solutions without added $[\text{emim}]\text{Cl}$ was below 0.003 M. In all other experiments it was below 0.006 M. The water concentration is specified for each particular experiment.

$[\text{emim}]\text{Cl}$ was obtained from Solvent Innovation and purified at least twice according to the following recrystallization procedure. $[\text{emim}]\text{Cl}$ (100 g) was dissolved in 10 mL of methanol and heated to about 60–70 °C until the salt was dissolved completely. Then it was allowed to cool down to ~50 °C, and 100 mL of cold, dried acetone was added. The mixture was stored at –30 °C overnight, and $[\text{emim}]\text{Cl}$ precipitated as a white solid. Afterward the remaining acetone was removed and the salt was dried under vacuum.

Instrumentation and Measurements. Karl Fischer titrations were done on a 756 KF Coulometer (Metrohm). Ion chromatography was performed on an Ion Chromatography System ICS-3000 (Dionex) IonPac AS20 with a GS20 guard column.²⁴

Thermodynamic Studies on the Reaction. The UV–vis spectra at ambient pressure were recorded on a Varian Cary 1G spectrophotometer equipped with a thermostated cell holder. In a typical experiment, deoxygenated $[\text{emim}][\text{OTf}]$ was saturated with NO in a gastight syringe.^{25,26} The NO solution was then mixed with a deoxygenated Fe(II) ionic liquid solution in a tandem cuvette in a 1:1 volume ratio. Fe(II) solutions were prepared by addition of FeCl_2 to $[\text{emim}][\text{OTf}]$, stirring the mixture overnight at 50 °C and in addition applying 30–60 min of ultrasonic treatment because of the poor solubility of the applied iron salt. The equilibrium constant K_{eq} was determined from absorbance changes measured at 473 nm in the temperature range 10–35 °C.

The pressure dependence of the equilibrium constant K_{eq} was measured between 5 and 150 MPa on a Shimadzu UV-2101 PC UV–vis spectrophotometer equipped with a custom-built high-pressure cell and the use of a quartz pill-box cuvette.²⁷ The high-pressure pump was purchased from NOVA SWISS²⁸ and enabled measurements in the selected pressure range. The measurements were carried out at 5 °C to slow down the decomposition of the nitrosyl complex during the time of the experiment. In all experiments, pressure cycles were performed to ensure that spectra collected during increasing pressure coincided exactly with spectra recorded during subsequent decreasing pressure.

In addition, K_{eq} for the studied nitrosylation reaction was determined in $[\text{emim}][\text{OTf}]$ solution with increased chloride content. In a typical experiment, Fe(II) solutions were prepared by adding FeCl_2 and $[\text{emim}]\text{Cl}$ to $[\text{emim}][\text{OTf}]$ in the ratio $[\text{Fe}^{2+}]/[\text{Cl}^-] = 1:7$ and stirring the mixture overnight at 45 °C. No further ultrasonic treatment or additional water was required to dissolve the employed salt. The preparation of the NO solution, subsequent mixing in a tandem cuvette, and determination of K_{eq} were performed as described earlier. The water content of the ionic liquid without and with added amounts of chloride was 0.007 and 0.04 M, respectively.

EPR Spectroscopy. Perpendicular mode EPR spectra were recorded on a JEOL continuous wave spectrometer JES-FA200 equipped with an X-band Gunn diode oscillator, a cylindrical mode cavity, and a liquid helium cryostat. The EPR measurements were performed in quartz tubes at 20 K. Data analyses were done with the JES-FA Series software package.

A solution of 0.0012 M FeCl_2 in deoxygenated ionic liquid was saturated with NO at 298 K in a gastight syringe and then rapidly filled into the EPR quartz tube. The solution was frozen by immersing the sample into liquid nitrogen before decomposition of the nitrosyl complex could start. The sample was afterward mounted into the EPR probe head that was placed into the precooled cryostat at 20 K. In addition, the spectra of a 0.0012 M FeCl_3 solution, a 0.0012 M FeCl_2 solution before saturation with NO, and a saturated NO solution in the deoxygenated ionic liquid were also recorded in the same manner

as described earlier to enable a better evaluation of the nitrosyl complex spectrum. The water content of the ionic liquid was 0.007 M.

IR Spectroscopy. IR spectra were recorded on an ATI Mattson FTIR Infinity spectrometer with the use of a CaF₂ cuvette (0.20 mm) for the pure ionic liquid and 0.08 M FeCl₂ ionic liquid solution before and after saturation with NO at 298 K. The Fe(II) solution was prepared by adding FeCl₂ and degassed water to the deoxygenated [emim][OTf] in the ratio 1:18 to achieve the necessary solubility of the iron salt. For every studied species, independent measurements of 50 scans were performed under inert gas atmosphere. The water content of the ionic liquid was 0.04 M.

Mössbauer Spectroscopy. ⁵⁷Fe Mössbauer spectra were recorded on a WissEl Mössbauer spectrometer (MRG-500) at 77 K in the constant acceleration mode. ⁵⁷Co/Rh was used as the radiation source. WinNormos for Igor Pro software was used for the quantitative evaluation of the spectral parameters (least-squares fitting to Lorentzian peaks). The minimum experimental line width was 0.20 mm s⁻¹. The temperature of the samples was controlled by an MBBC-HE0106 MÖSSBAUER He/N₂ cryostat within an accuracy of ±0.3 K. Isomer shifts were determined relative to α-iron at 298 K. Experimentally obtained spectra of the solutions without an excess of chloride were simulated with the MFIT Simulation Program, version 1.1, E. Bill, MPI for Bioinorganic Chemistry, Mülheim an der Ruhr, Germany.

The following samples were measured before and after saturation with NO: (i) a solution of 0.06 M ⁵⁷FeCl₂ in deoxygenated [emim][OTf] with an added 18-fold amount of degassed water to achieve the necessary solubility of the iron salt; (ii) a solution of 0.06 M ⁵⁷FeCl₂ in deoxygenated [emim][OTf] with added [emim]Cl and degassed water resulting in a 7-fold excess of chloride and 18-fold excess of water over iron(II); and (iii) a solution of 0.06 M ⁵⁷FeCl₂ in deoxygenated [emim][OTf] with added [emim]Cl resulting in a 7-fold excess of chloride over iron(II) ions but without adding extra water. The water content of the ionic liquid itself, viz. (i) 0.04 M with additional water, (ii) 0.1 M with additional [emim]Cl and water, and (iii) 0.003 M with additional [emim]Cl, was taken into account in preparing the described solutions. All solutions prepared at room temperature were rapidly filled into the Teflon container placed in the brass inlet. The solutions were frozen by immersing the samples into liquid nitrogen before the oxidation of the dissolved iron(II) compound to iron(III) or the decomposition of the nitrosyl complex could start. The samples were afterward mounted into the Mössbauer probe head that was placed into the precooled cryostat at 77 K. The spectrum of solid [emim]₂[FeCl₄] was recorded in a similar way.

X-ray Crystal Structure Determination. [emim]₂FeCl₄ was synthesized from FeCl₂ (318 mg, 2.51 mmol) and [emim]Cl (1.83 g, 12 mmol), both dissolved in 2.5 mL of deoxygenated [emim][OTf] containing 0.04 M water by stirring under vacuum at 44 °C overnight. The clear brownish solution was placed in the refrigerator (4 °C), and colorless crystals formed after 4 days that were suitable for X-ray analysis; the molecular weight was 419.99 g/mol. A block-shaped crystal of approximately 0.32 × 0.21 × 0.16 mm³ in size was covered with protective perfluoropolyalkylether oil and transferred into the cold N₂ gas stream of the diffractometer. Intensity data of the crystal were collected at 150(2) K on a Bruker Kappa APEX 2 IμS Duo diffractometer using focusing QUAZAR Montel optics (Mo Kα radiation, λ = 0.71073 Å). Data were corrected for Lorentz and polarization effects, and semiempirical absorption corrections were performed on the basis of multiple scans using SADABS.²⁹ The structure was solved by direct methods and refined by full-matrix least-squares procedures on F² using SHELXTL NT 6.12.³⁰ All non-hydrogen atoms were refined with anisotropic displacement parameters. The hydrogen atoms were placed in positions of optimized geometry, and their isotropic displacement parameters were tied to those of the corresponding carrier atoms by a factor of 1.2 or 1.5. CCDC-778167 contains the supplementary crystallographic data for this structure. These data can be obtained free of charge from The Cambridge Crystallographic Data Centre via www.ccdc.cam.ac.uk/data_request/cif.

RESULTS AND DISCUSSION

Studies on NO activation by transition metal complexes has a long tradition in our group.³¹ In a series of studies, detailed mechanistic investigations on the interaction of NO with a series of polyaminocarboxylate complexes of Fe(II) in aqueous solution were performed.³² Furthermore, we verified the mechanistic details of the underlying reaction in the absence of chelating ligands, the so-called “brown ring” test reaction for nitrate, and the nature of the reaction product [Fe-(H₂O)₅NO]²⁺ was clarified, an aspect that provoked considerable discrepancies in the literature before.³³ In a subsequent study, we extended our investigations to a mechanistic survey of the classic brown ring reaction in an IL and selected 1-ethyl-3-methylimidazolium dicyanamide, [emim][dca], as the reaction medium for which the anion exhibits a strong donor ability.¹⁹ The displacement of the aqueous by the IL medium caused several changes in the reaction mechanism caused by a completely modified structure of the dissolved Fe(II) species in solution.

It is well-known that, on dissolving FeCl₂ in water, [Fe(H₂O)₆]²⁺ is formed in weakly acidic solution. By a subsequent reversible reaction with NO, one of the water ligands is displaced by NO to form the characteristic green–brown [Fe(H₂O)₅NO]²⁺ complex, which is responsible for the formation of the brown ring. The transfer of this reaction from an aqueous to an IL medium revealed questions concerning the structure of the ferrous reactant and product species, because the situation becomes significantly more complicated in an IL. In the case of [emim][dca], there are three potential ligands present in the IL, viz. chloride ions from FeCl₂ used as Fe(II) source, water molecules present in the very hygroscopic IL despite thorough drying, and the high concentration of dca anions present in the IL, which are known for their strong coordination ability.^{34,35} The crystal structure of the ferrous complex isolated from the IL helped to clarify the situation. It revealed a coordination polymer of Fe(II) complexes, where every metal center exhibits a distorted octahedral coordination sphere, formed by one chloride and five dca⁻ ligands in end-on and side-on coordination modes. A series of IR measurements performed in solutions of varying concentrations of iron(II) species, as well as in the solid state, enabled us to show that the monomeric [Fe(dca)₅Cl]⁴⁻ complex is present in the IL medium (see Figure 1) and undergoes a reaction with NO during which chloride is displaced to form the nitrosyl product

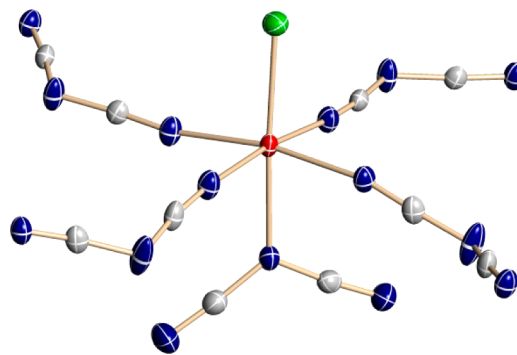


Figure 1. Structural information on the monomeric Fe(II) complex present in the [emim][dca] solution (50% probability ellipsoids: red, Fe; green, Cl; blue, N; gray, C).¹⁹

{Fe–NO}⁷. Formally, the product has a Fe^{III}–NO[−] character as in the case of an aqueous medium.

Thus, both investigated solvents, water and [emim][dca], exhibit appreciable donor strength and provide ligands, solvent molecules (H₂O), or anions (dca[−]) to form the coordination sphere of the metal center that is required to dissolve FeCl₂ in the IL. For this reason FeCl₂ turned out to be readily soluble in [emim][dca] through formation of the [Fe(dca)₅Cl]^{4−} complex.

Apparently, the situation will be significantly different in [emim][OTf], because OTf[−] is a very weak donor and the main questions are whether and in what form FeCl₂ will dissolve in this IL? We found that FeCl₂ has a very poor solubility in [emim][OTf] because the triflate anions, present in a very large excess, are not able to provide an effective coordination sphere for the metal center. The observed weak solubility could be ascribed to the presence of a marginal concentration of chloride ions that remained in the IL from the synthetic route and especially water in the hygroscopic IL. Furthermore, we found a correlation between the solubility of FeCl₂ and the water content of the IL. This suggested the presence of water and/or chloride ligands in the coordination sphere of the dissolved FeCl₂, although it was not possible to verify our suggestion by the isolation of any compound suitable for X-ray analysis.

Work in Neat [emim][OTf]. We started our studies in neat [emim][OTf], i.e., we purified the IL as well as we could in the way described earlier. Our initial investigations demonstrated that the nitrosylation reaction on the Fe(II) center occurs successfully in [emim][OTf] as medium and the formation of the nitrosyl complex is completely reversible, which was tested by alternatively bubbling NO and N₂ through the precursor complex solution. The spectrum of the precursor complex in [emim][OTf] exhibits no absorption band between 300 and 800 nm, whereas the nitrosylated species shows a two-band maxima (see Figure 2) shifted to higher wavelength depending on the applied solvent (see Table 1).

A collection of broad medium-intense ($\epsilon < 2000 \text{ M}^{-1} \text{ cm}^{-1}$) features between 300 and 700 nm in the absorption spectra is characteristic for the majority of high-spin nonheme iron-nitrosyls.³⁶ Two of the bands around 340 and 440 nm, respectively, were attributed to ligand-to-metal charge-transfer

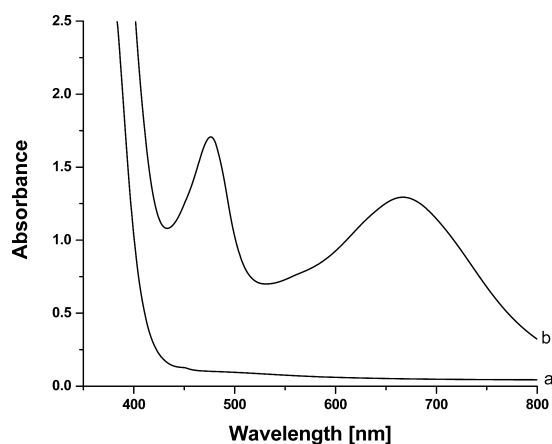


Figure 2. Absorption spectral changes recorded for the reaction of 0.01 M Fe(II) precursor complex with NO in [emim][OTf] at room temperature. Curves: precursor complex solution (trace a); precursor complex solution saturated with NO (trace b).

Table 1. Comparison of the UV-Vis Data and Equilibrium Constants of the Nitrosylated Fe(II) Complex in Different Solvents

solvent	band position ^a [nm]		K_{eq} [M ^{−1}]
water	451 (265)	585 (85)	1150 ± 50 ^b
			440 ± 110 ^c
[emim][dca]	465 (156)	627 (35)	172 ± 20
[emim][OTf]	473 (198)	665 (80)	420 ± 70

^aMolar extinction coefficients are quoted in brackets in M^{−1} cm^{−1}.

^bThermodynamically obtained value. ^cKinetically obtained value.

transitions (LMCT), whereas the one at lower energy around 600 nm was ascribed to a d-d transition. A series of iron-nitrosyl complexes with iron chelated by polyaminocarboxylate ligands was extensively studied in our group.^{32a} These studies revealed that the stability of the nitrosyl complexes is controlled by their ability to bind NO as {Fe^{III}–NO[−]}, which correlated with the position of the LMCT band, viz. a synchronous increase in the band energy and complex-formation constant was observed. On the basis of these considerations, it was concluded that one of the most stable nitrosyl complexes of the series studied, viz. the [Fe(edta)(NO)]^{2−} complex for which $K_{\text{eq}} = (2.05 \pm 0.15) \times 10^6 \text{ M}^{-1}$, demonstrated a pronounced {Fe^{III}–NO[−]} charge distribution, whereas the [Fe(H₂O)₅(NO)]²⁺ complex tended to be more of the Fe^{II}–NO[•] type, although the Mössbauer spectrum clearly favored the Fe^{III}–NO[−] formulation.³³

The shift in the LMCT band to higher wavelengths observed for both ILs correlates with significantly lower complex-formation constants found for the nitrosylation reaction in these solvents. The lower intensity of the CT bands (see Table 1) compared to those found in aqueous medium suggests less importance of charge transfer between the NO ligand and the Fe center in the presented complexes. In addition, the more intense ($\epsilon = 80 \text{ M}^{-1} \text{ cm}^{-1}$) d-d band relative to the CT band ($\epsilon = 198 \text{ M}^{-1} \text{ cm}^{-1}$) in [emim][OTf] compared to the other solvents^{32a} underlines the stronger Fe^{II}–NO[•] character of the iron-nitrosyl bond. Recent theoretical calculations using a multiconfigurational CASSCF/CASPT2 approach suggest that the nature of the Fe–NO bond in {FeNO}⁷ complexes can be best understood in terms of contributions from a mixture of Fe^{II}–NO[•] and Fe^{III}–NO[−] resonance structures.³⁷ Crystal structures for some nonheme {FeNO}⁷ complexes show a similar trend,³⁸ where the more recent work reported evidence for the presence of high-spin Fe(III) ($S = 5/2$) antiferromagnetically coupled to NO[−] ($S = 1$).

The complex-formation constant at room temperature was determined by performing a spectrophotometric titration for the nitrosylation reaction by following the change in absorbance (ΔAbs) at 473 nm for mixing various concentrations of the Fe(II) complex with NO as shown in Figure 3. K_{eq} was calculated according to eq 1, where A_0 and A_{∞} represent the absorbance of the precursor complex and nitrosyl product, respectively, and A_x is the absorbance at any Fe(II) complex concentration. From the data in Figure 3, K_{eq} was found to be $420 \pm 70 \text{ M}^{-1}$. As shown in Table 1, this value lies between those found in [emim][dca] and water as solvents if we take the thermodynamically determined value for water into account, but it is very close to the kinetically determined value in water. This can be considered as a further indication that water molecules participate in the formation of the coordination sphere of the iron complex upon dissolving FeCl₂ in

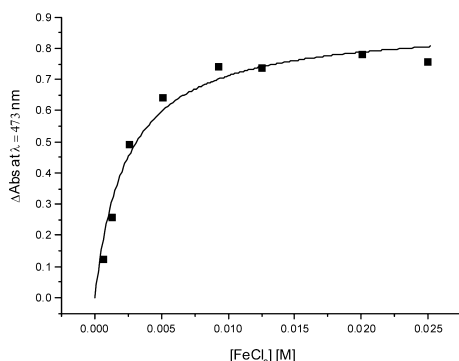


Figure 3. Change in absorbance at 473 nm for the reaction of the Fe(II) complex with NO in [emim][OTf] as a function of the FeCl₂ concentration. Experimental conditions: *c*(NO) = 7 mM, *T* = 25 °C.

[emim][OTf] as medium, thus affecting the equilibrium of the nitrosylation reaction.

$$A_x = A_0 + \frac{(A_\infty - A_0)K_{\text{eq}}[\text{Fe}^{\text{II}}]}{1 + K_{\text{eq}}[\text{Fe}^{\text{II}}]} \quad (1)$$

The influence of temperature (in the range 10–35 °C) and pressure (up to 150 MPa and at 5 °C to prevent decomposition of the nitrosyl complex) on the equilibrium was studied to determine the standard reaction parameters for the nitrosylation reaction. A linear plot of $\ln(K_{\text{eq}})$ vs $1/T$ enabled the determination of $\Delta H^\circ = -6.0 \pm 0.3 \text{ kJ mol}^{-1}$ and $\Delta S^\circ = +30 \pm 1 \text{ J K}^{-1} \text{ mol}^{-1}$ from the slope and intercept, respectively, according to eq 2. The results demonstrate that decomposition of the nitrosyl product is favored on increasing temperature according to an exothermic reaction for which ΔH° has a negative value. According to eq 3, a linear fit of $\ln(K_{\text{eq}})$ vs pressure allowed the determination of $\Delta V^\circ = -0.8 \pm 0.1 \text{ cm}^3 \text{ mol}^{-1}$. This shows that increasing pressure favors the formation of the nitrosyl complex, i.e., increasing temperature and pressure have opposite effects on the coordination of NO to the Fe(II) center in [emim][OTf].

$$R \ln K_{\text{eq}} = -\frac{\Delta H^\circ}{T} + \Delta S^\circ \quad (2)$$

$$\ln K_{\text{eq}} = -\frac{P}{RT} \Delta V^\circ \quad (3)$$

Our results demonstrate that temperature and pressure variations have only a small influence on the studied equilibrium in [emim][OTf] as solvent. The calculated standard reaction parameters are summarized in Table 2 and compared with the data obtained earlier in the other solvents. In all three cases, formation of the Fe(II)-nitrosyl complex occurs in a reversible exothermic process with similar enthalpy values in [emim][OTf] and water.

The significantly positive value of the standard reaction entropy in [emim][OTf] can be ascribed to the poor

Table 2. Standard Reaction Parameters for the Formation of the Fe(II)-Nitrosyl Complex in Different Solvents

solvent	[emim][OTf]	[emim][dca] ¹⁹	water ³³
ΔH° [kJ mol ⁻¹]	-6.0 ± 0.3	-37 ± 1	-11 ± 2
ΔS° [J K ⁻¹ mol ⁻¹]	$+30 \pm 1$	-81 ± 4	$+12 \pm 6$
ΔV° [cm ³ mol ⁻¹]	-0.8 ± 0.1	-7.5 ± 0.2	$+4.8 \pm 0.6$

stabilization of the resulting nitrosyl complex in this medium compared to [emim][dca], where ΔS° has a large negative value. The observed difference is likely associated with the varying chemical nature of the iron complex in the different ILs. In [emim][dca] the Fe center is coordinated to five dca⁻ ligands (see Figure 1) and thus is well incorporated in the bulk of the solvent, leading to a decrease in entropy. In the case of [emim][OTf], the iron center coordinates most likely only to Cl⁻ and water ligands and not to the IL's anion. Therefore, the metal complex lacks the manifold of interactions with the solvent and the consequential stabilization present in the other IL, hence resulting in a large positive value for ΔS° .

Subsequently we applied different spectroscopic methods that proved to be successful in our previous attempts to characterize the nitrosyl product, viz. IR, EPR, and Mössbauer spectroscopy. IR spectroscopy is in general considered to be a useful tool for the determination of the bonding mode and oxidation state of NO in metal-NO complexes.³⁹ According to the literature, free NO in solution does not exhibit any absorption bands that are readily detectable in the relevant window of the spectrum.⁴⁰ FTIR measurements of [emim][OTf] solutions using a CaF₂ cuvette provided better results than those obtained by attenuated total reflection IR (ATR-IR) spectroscopy, as was already the case in [emim][dca] as solvent.¹⁹ Spectra of the Fe(II) solution before and after saturation with NO were measured at room temperature and are presented in Figure 4.

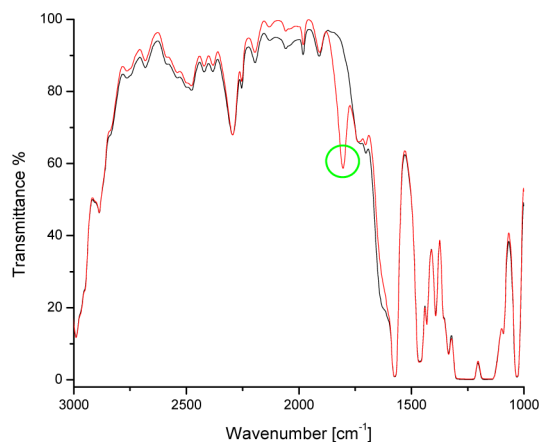


Figure 4. IR spectra of the Fe(II) (black line) and nitrosylated Fe(II) solution (red line) in [emim][OTf] at room temperature. Experimental conditions: 0.08 M Fe(II) solution saturated with NO at 298 K, $\bar{\nu} = 1804 \text{ cm}^{-1}$ (m, NO).

The formation of a single peak at 1804 cm^{-1} was clearly observed, indicating the formation of the iron-nitrosyl complex. This value is very similar to that found in aqueous solution; see Table 3. In the case of water as medium, the explanation for the electronic distribution between the iron center and the NO ligand was based on the results gained from IR measurements

Table 3. Comparison of the Peak Positions in the IR Spectrum Originating from the Iron-Nitrosyl Complex in Different Solvents

solvent	water ³³	[emim][OTf]	[emim][dca] ¹⁹
position in spectrum [cm ⁻¹]	1810	1804	1767
acceptor number ⁴¹	54.8	37.1	31.7

on iron(II) polyaminocarboxylate complexes obtained before in our group^{32a} and supported the presence of a species formally written as $\{\text{Fe}^{\text{III}}-\text{NO}^-\}$.

For the high-spin $\{\text{Fe}^{\text{III}}-\text{NO}^-\}$ systems, the strength of the Fe–NO and N–O bonds is strongly influenced by the effective nuclear charge on iron.³⁶ In such systems the nitroxyl unit behaves as a relatively weak π -acceptor but a strong π -donor. In a complex with an anionic set of ligands, the effective nuclear charge on iron is decreased and lowers π -donation from the NO⁻ orbitals. This leads to weaker N–O and Fe–NO bonds and thus lowers the NO stretching frequency. Displacement of the anionic by neutral ligands increases the effective charge on iron, which is compensated by an increased donation from the NO⁻ ligand. The NO stretching frequencies of 1810 cm⁻¹ in water and 1767 cm⁻¹ in [emim][dca] as medium are in good agreement with such considerations because the iron center is coordinated only to neutral (water molecules) or anionic (dca⁻ and Cl⁻) ligands, respectively.

On the other hand, the NO stretching frequency correlates with the solvent polarity, expressed by acceptor number (AN) of the solvent.⁴² AN is a measure of the solvent's electrophilic properties, namely, the ability to accept electron pairs or at least electron density.⁴³ The acceptor numbers for a series of ionic liquid were recently determined in our group,⁴¹ and the values for [emim][dca], [emim][OTf], and water are included in Table 3. Previous detailed investigations utilizing sodium nitroprusside as a model complex revealed that the transfer of electron density from the negatively charged ligands to the solvent promotes the flow of electron density from the metal center to the ligands. This, on the one hand, decreases the π -back-bonding interaction of the Fe and nitrosyl ligand and, on the other hand, increases π donation from the nitrosyl ligand to Fe, resulting in an increase in the strength of the N–O bond and a higher NO stretching frequency.⁴² Accordingly, the solvent with higher AN can stabilize the N–O bond even in a complex with an anionic set of ligands.

A similar effect may be valid in the studied IL. Although the Fe is coordinated mostly by anionic ligands (Cl⁻) and thus the NO stretching frequency should resemble the value in [emim][dca], the AN of [emim][OTf] is higher such that the solvent stabilizes the negative charge of the ligands and consequently the NO stretching frequency increases.

Hence, the IR data for the iron-nitrosyl complex in [emim][OTf] solution supplement the UV–vis data and provide direct evidence for the coordination of NO to the Fe(II) center. Once again, the obtained results are more similar to those found in aqueous solution, from which we conclude that at least a part of the coordination sphere of the iron center is occupied by water molecules.

The X-band EPR spectrum of the nitrosylated Fe(II) complex was measured in frozen solution at 20 K as shown in Figure 5. The spectrum reveals at least two species present in a frozen solution. The very asymmetric broad signal centered at about $g = 1.98$ is typical for “free” NO molecules in frozen solution. The low g value and the large width of this $S = 1/2$ spectrum indicate the presence of substantial spin–orbit interaction, as expected for the NO radical. The low-field part of the spectrum together with a signal at $g = 2.04$ could be assigned to the iron-nitrosyl complex with g values of 4.05, 4.05, and 2.04, which are typical of a spin quartet species ($S = 3/2$) with dominating zero-field splitting, $D \gg h\nu$ (0.3 cm⁻¹ at X-band), and vanishing rhombicity, $E/D = 0$. These signals found in [emim][OTf] as medium are of a much lower intensity than

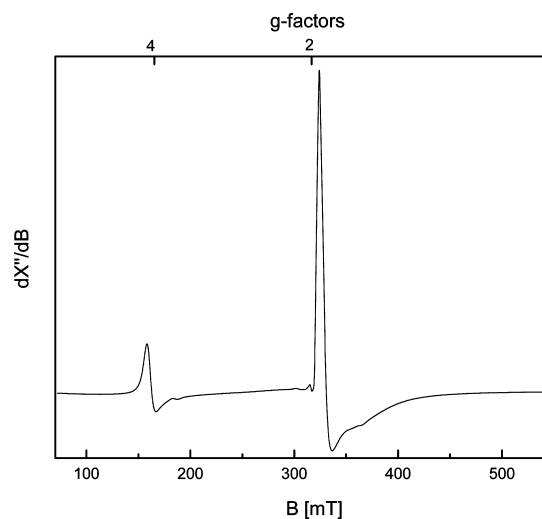


Figure 5. X-band EPR spectrum of the nitrosylated Fe(II) solution in [emim][OTf]. Experimental conditions: 0.0012 M Fe(II) solution saturated with NO at 298 K, measuring temperature 20 K, microwave frequency 8.9858 GHz, power 1 mW, and modulation 1.0 mT at 100 kHz.

those observed in [emim][dca], but are otherwise very similar to them. Related spectra are also presented in the literature for solutions of $[\text{Fe}(\text{edta})(\text{NO})]^{44}$ or $[(1,4,7\text{-trimethyl-1,4,7-triazacyclononane})\text{-Fe}(\text{NO})(\text{N}_3)_2]^{45}$ or $[\text{Fe}(\text{H}_2\text{O})_5\text{NO}]\text{Cl}_2$.³³ In general, EPR spectra of high-spin nonheme $\{\text{Fe}-\text{NO}\}^7$ complexes typically show effective g values very close to $g \approx 4$ and $g \approx 2$, indicative of an $S = 3/2$ total spin.³⁶ Hence, the subspectrum assigned to the iron-nitrosyl product confirms the $S = 3/2$ ground state of the $\{\text{FeNO}\}^7$ core.

Mössbauer spectroscopy is known to be very helpful to distinguish between oxidation and spin states of the iron center. The zero-field Mössbauer spectra of $^{57}\text{FeCl}_2$ dissolved in [emim][OTf] containing added water to improve solubility of the iron salt were measured in frozen solution at 77 K before and after the reaction with NO and turned out to be very complex. The obtained parameters and species suggested to be present in the investigated solutions are summarized in Table 4.

The spectrum of the Fe(II) solution prior to nitrosylation can be deconvoluted into two overlapping quadrupole doublets with only a small ($\sim 10\%$) difference in relative intensities. The doublet with the higher intensity shows a very large isomer shift (1.38 mm/s), typical of high-spin Fe(II) coordinated to oxygen-donor ligands (e.g., water).^{46,33} The corresponding quadrupole splitting is also large; see Table 4. On the basis of these results, we suggest that the species is the high-spin $[\text{Fe}(\text{H}_2\text{O})_6]^{2+}$ complex, which can be formed in [emim][OTf] solution because a considerable amount of water was added to the ionic liquid to increase the solubility of the starting iron salt ($^{57}\text{FeCl}_2$) to reach the high concentration required for the Mössbauer experiment. The second doublet also demonstrates a high isomer shift and quadrupole splitting, typical of high-spin Fe(II) in a 4- to 6-fold oxygen-rich coordination environment, containing also other ligands, e.g., chloride. Similar values are also known from the literature.⁴⁷ These results are consistent with our initial assumptions: because triflate anions apparently do not provide a strong enough coordination environment for the metal center, the solubility of the iron salt is poor, until some water is added. These water molecules, along with the chloride ions originating from the employed salt ($^{57}\text{FeCl}_2$),

Table 4. Summary of the Isomer Shifts (IS), Quadrupole Splittings (QS), and Relative Intensities of the Species Likely to Be Present in the $^{57}\text{FeCl}_2$ Solutions of [emim][OTf], before and after Nitrosylation

	precursor, without NO		after saturation with NO		
IS, mm/s	1.38	1.19	1.40	1.15	1.13
QS, mm/s	3.40	2.60	3.44	2.70	0.03
relative intensity, %	54.7	45.3	53.4	18.5	28.1
presumable species	$[\text{Fe}(\text{H}_2\text{O})_6]^{2+}$	$[\text{FeCl}_x(\text{H}_2\text{O})_y]^n$, $x = 4, y = 1, 2$	$[\text{Fe}(\text{H}_2\text{O})_6]^{2+}$	$[\text{FeCl}_x(\text{H}_2\text{O})_y]^n$, $x = 4, y = 1, 2$	Fe(II) h.s. species

form the coordination sphere of the iron species present in the ionic liquid solution prior to the nitrosylation reaction.

The spectrum recorded following saturation of the Fe(II) solution with NO can be simulated when the presence of three different species is assumed. The one with the largest isomer shift and quadrupole splitting still accounts for ca. 50% of the overall relative intensity and can be assigned to the high-spin $[\text{Fe}(\text{H}_2\text{O})_6]^{2+}$ complex, which seems to be unaltered by the presence of NO. The second species with the lower isomer shift and quadrupole splitting resembles the high-spin Fe(II) complex with mixed chloro and aqua ligands that was present in the solution before the nitrosylation, although it now accounts for ca. 20% of the overall relative intensity. The residual 30% presents the third component that was formed during nitrosylation as it was not present in the mixture before. The isomer shift is again typical for a high-spin Fe(II) center in a 4- to 6-fold coordination environment. However, this species is very unusual due to the extremely low quadrupole splitting: 0.03 mm/s. There are only a few examples of iron-containing species with similarly small quadrupole splitting published to date, e.g., the Fe(III)⁴⁸ or Fe(II)^{49,46a} species with chloro and/or aqua ligands or Fe(II) species with nitrogen ligands.⁵⁰ In all these cases, such a small value or even the lack of the quadrupole splitting was ascribed to an ideal symmetric coordination environment and in consequence a minimal electric field gradient at the metal center. Adopting this explanation to our case implies a high local symmetry around the iron center, which more likely requires only one type of ligand. However, if the studied species is a result of nitrosylation, at least one of the ligands should be NO. Apparently the nature of the nitrosylation product is more complicated as to be deciphered only by means of Mössbauer spectroscopy.

Effect of Added Chloride to [emim][OTf]. Our results demonstrate that, under the selected experimental conditions, the ionic liquid solution contains different species, which complicates the exploration of the situation. In an effort to simplify the matter and to increase the ratio of chloride coordinated species, we increased the chloride content of the solution by adding [emim]Cl at otherwise unchanged conditions. This attempt was very successful in different respects. This time we were able to isolate crystals of the ferrous complex suitable for X-ray analysis.

On dissolving FeCl_2 and [emim]Cl in the ratio $\text{Fe}^{2+}/\text{Cl}^- = 1:7$ in [emim][OTf], colorless crystals precipitated at low temperature (4 °C) which turned out to be the tetrachloridoferrate(II) complex with two [emim]⁺ cations for charge neutralization, [emim]₂[FeCl₄]. The crystal structure was resolved at 150 K; the crystal belongs to the tetragonal system, space group I 41/a ($Z = 8$) (see Table 5 for further crystallographic data).

Tetrachloridoferrate complexes of Fe(II) or Fe(III) with large organic or organometallic cations are known from the literature,^{51,52} but as far as we know there is no evidence for

Table 5. Crystallographic Data for [emim]₂FeCl₄ Collected at 150 K (Estimated Standard Deviations in the Last Significant Digits Are Given in Parentheses)

empirical formula		$\text{C}_{12}\text{H}_{22}\text{Cl}_4\text{FeN}_4$	
M [g mol ⁻¹]		419.99	
system		tetragonal	
space group		I 41/a	
<i>a</i> [Å]	α [°]	14.1040(9)	90
<i>b</i> [Å]	β [°]	14.1040(9)	90
<i>c</i> [Å]	γ [°]	19.239(2)	90
<i>V</i> [Å ³]	<i>Z</i>	3827.1(5)	8
crystal size [mm ³]		0.32 × 0.21 × 0.16	
ρ_{calc} [g cm ⁻³]		1.458	
$\mu(\text{Mo K}\alpha)$ [mm ⁻¹]		1.345	
<i>F</i> (000)		1728	
θ range [°]		2.89–29.50	
reflections collected		41508	
independent reflections, R_{int}		2680, 0.0398	
independent reflections with $I > 2\sigma(I)$		2677	
parameters refined		96	
max. transmission	min. transmission	0.8136	0.6729
$R_1[F^2 > 2\sigma(F^2)]$		0.0389	
$wR_2(F^2)$		0.1155	
Goodness-of-fit on F^2		1.091	

such complexes obtained directly from IL media. Crystal structures of tetrachloridometallates of transition metal ions with dialkylimidazolium cations, e.g., [emim]₂[CoCl₄] and [emim]₂[NiCl₄], are known.⁵³ They were obtained to gain more information about the structure of ambient-temperature ILs; however, the solids were isolated not from an IL medium but from conventional solvents. Considerable attention in recent literature was given to ionic liquids containing tetrachloridoferrate(III) due to their noticeable magnetic properties.⁵⁴ In addition, there are examples of FeCl₃- and FeCl₂-based ionic liquids,⁵⁵ obtained by mixing with [bmim]Cl similar to the AlCl₃-containing ILs,⁵⁶ which at that time resulted in growing interest in research in the field of ionic liquids. However, these studies did not report any crystal structures of tetrachloridoferrate(II) complexes. Furthermore, the numerous studies in which transition metal chlorides were placed in ionic liquids for a variety of purposes were reviewed in 1988.⁵⁷ There are investigations on the behavior of molybdenum,⁵⁸ titanium,⁵⁹ copper,⁶⁰ nickel, and iron⁶¹ chlorides. In all these cases, visible absorption spectroscopy or more often electrochemical techniques were applied to characterize the complexes.

Some examples of coordination compounds with the in principle weakly coordinating [OTf]⁻ anion are known from the literature,⁶² but as expected no coordination to the metal center occurs in the presence of more strongly coordinating ligands.⁶³ A similar situation was observed in our case: no OTf⁻ is present in the structure and every iron center is coordinated

by only four chloride ions, giving the tetrachloridoferrate anion. Furthermore, we discovered a slight disorder in the ethyl group of the $[\text{emim}]^+$ cation (see Figure 6), which is neglected in the subsequent discussion because the prevailing interactions include mainly the hydrogen atoms bound directly to the imidazole ring.

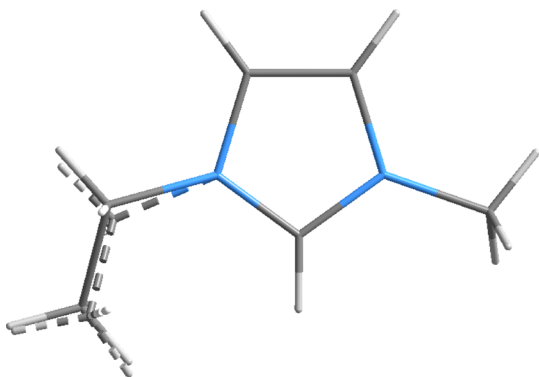


Figure 6. $[\text{emim}]^+$ cation showing the disorder of the ethyl group.

The ions are packed in the unit cell as shown in Figure 7. The geometry of $[\text{FeCl}_4]^{2-}$ is that of a slightly distorted

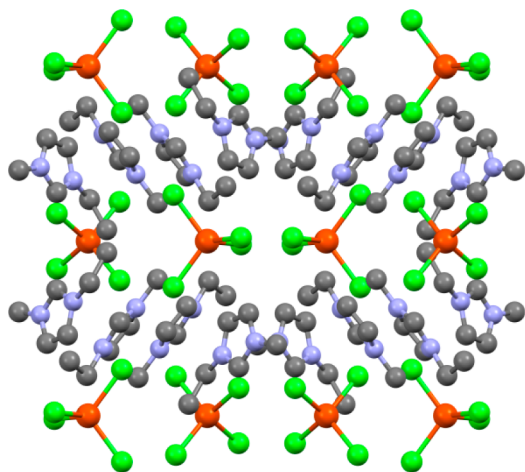


Figure 7. View of the unit cell of $[\text{emim}]_2[\text{FeCl}_4]$ along the b -axis. The a -axis is vertical, and the c -axis is horizontal. Red denotes Fe atoms, green denotes Cl atoms, blue denotes N atoms, and gray denotes C atoms; H atoms are omitted for the sake of clarity.

tetrahedron with bond angles ranging from a low of 107.81° to a high of 110.31° . The four intramolecular Fe–Cl bond distances of 2.32 \AA are in good agreement with the values reported for the tetramethylammonium tetrachloridoferrate(II) complex (average value of 2.29 \AA)⁵¹ and are considerably longer than the Fe(III)–Cl distances (average value of 2.19 \AA),⁵² as expected for the high-spin Fe(II) center. The shortest Fe–Fe distances between the $[\text{FeCl}_4]^{2-}$ anions with 8.536 \AA are somewhat longer than in the case of high-spin iron(II) bridged complexes^{19,64} (values from 8.119 to 8.414 \AA).

In a survey of neutron diffraction data, Taylor and Kennard⁶⁵ have demonstrated, using the values of 0.12 and 0.175 nm for the van der Waals radii of hydrogen and chlorine atoms, respectively, that a contact shorter than 0.295 nm reliably indicates the presence of a $\text{C}\cdots\text{H}\cdots\text{Cl}$ hydrogen bond. This kind of nonclassical hydrogen bonding is a type of weak

intermolecular interaction that plays an important role in crystal packing⁶⁶ and was also found in the present structure. The local structure around a single cation is shown in Figure 8.

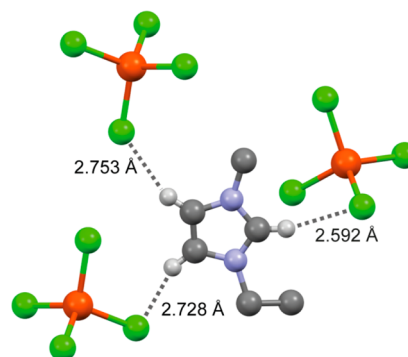


Figure 8. Local structure around a single cation in $[\text{emim}]_2[\text{FeCl}_4]$.

All three hydrogen atoms of the imidazolium ring are involved in significant hydrogen-bonding interactions with three different $[\text{FeCl}_4]^{2-}$ anions, with the shortest contact of 2.592 \AA arising for the H(1) and somewhat longer contacts of 2.728 and 2.753 \AA for the H(2) and H(3) atoms, respectively. These values are in good agreement with those found for the similar structures of $[\text{emim}]_2[\text{MCl}_4]$, $\text{M} = \text{Co}, \text{Ni}$ ⁵³ (2.56 – 2.59 \AA for H(1) and 2.63 – 2.84 \AA for H(2,3)).

Two crystallographically distinct anions were found in the structure, with hydrogen bonding to either H(1) protons (see Figure 9) or H(2) and H(3) (see Figure 10) protons of the

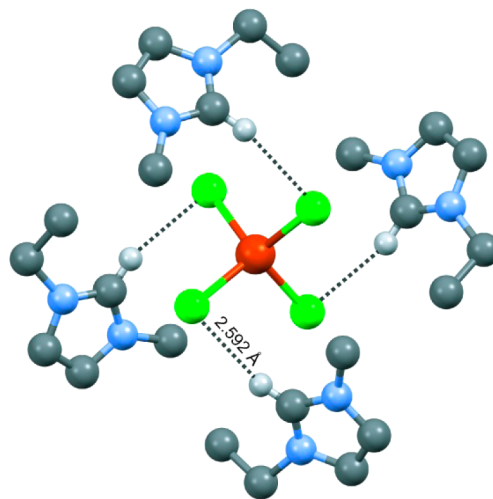


Figure 9. Local structure around a single anion in $[\text{emim}]_2[\text{FeCl}_4]$. All depicted $\text{Cl}\cdots\text{HC}$ distances are equivalent.

imidazolium ring, but not to both. Nevertheless, all the chlorine atoms of the anion are involved in a complex three-dimensional hydrogen-bonding network. In addition, we found a hydrogen-bonded ring structure (see Figure 11), reminiscent of that reported elsewhere.^{53,67}

An earlier contribution reported that, when the chlorine atom is hydrogen bonded to a cation, the mean $\text{M}\cdots\text{Cl}$ bond length is longer.⁵³ The authors compared the bond lengths for the tetrachloridometallate(II) complexes with the $[\text{emim}]^+$ cation, for which they detected hydrogen-bond interaction with the anion or with the tetramethylammonium cation, for

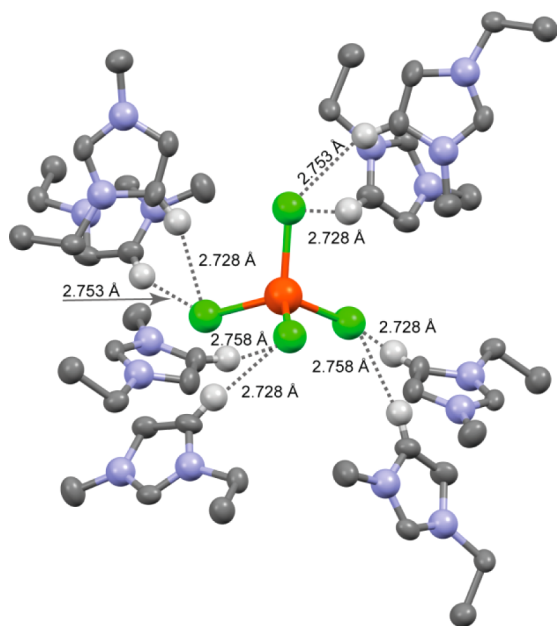


Figure 10. Local structure around a single anion in $[\text{emim}]_2[\text{FeCl}_4]$.

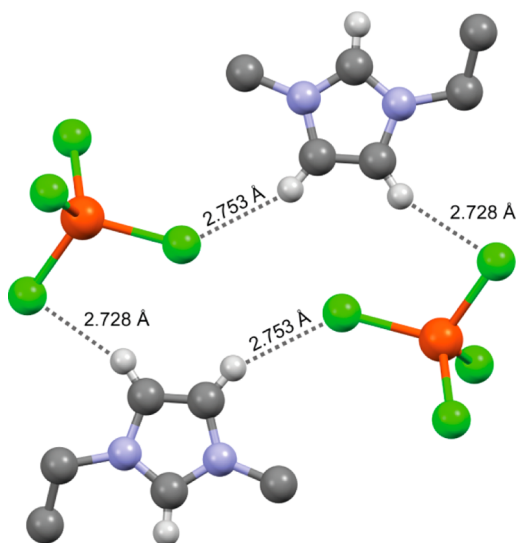


Figure 11. Hydrogen-bonded ring structure in $[\text{emim}]_2[\text{FeCl}_4]$.

which no hydrogen bonding was either claimed or expected, and found a difference of ~ 0.02 Å for both Co and Ni centers. On comparing the Fe–Cl bond lengths in our compound (2.315 Å) with the corresponding tetramethylammonium salt⁵¹ (2.292 Å), we noted nearly the same difference of 0.023 Å.

The described observations concerning the extensive hydrogen-bond interactions between the cations and the anions demonstrate that the isolated $[\text{emim}]_2[\text{FeCl}_4]$ species cannot be described as a simple collection of ion pairs. All ring protons and all chlorine atoms of the anions are involved in an extended three-dimensional hydrogen-bonding network. Furthermore, the detected Fe–Cl bond lengths are in line with the values expected for a high-spin Fe(II) center.

In addition, we performed Mössbauer spectroscopy on the obtained solid $[\text{emim}]_2[\text{FeCl}_4]$ at 77 K; see Figure 12. The resulting spectrum shows only one doublet with the quadrupole splitting (2.10 mm/s) and especially the isomer shift (1.05 mm/s) typical for a tetrachloridoferrate(II) complex with a

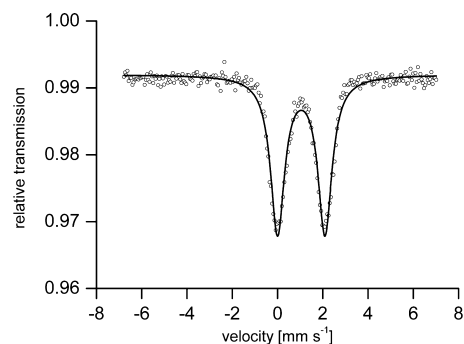


Figure 12. Zero-field Mössbauer spectrum of the solid $[\text{emim}]_2[\text{FeCl}_4]$ at 77 K.

high-spin Fe(II) center in a tetrahedral environment, well-known from the literature.⁶⁸

The structure of the metal species present in solution can differ from the one found in the solid state, as was the case for the iron complex studied in $[\text{emim}][\text{dca}]$ as medium before.¹⁹ For example, additional water molecules can coordinate to the metal center upon dissolving it in $[\text{emim}][\text{OTf}]$. Further investigations are required to verify the nature of the dissolved iron complex.

On the basis of this success, we performed zero-field Mössbauer measurements in the frozen IL solution (77 K) with increased chloride content and varying water concentration before and after the nitrosylation reaction. The obtained parameters, as well as the species likely to be present in the investigated solutions, are summarized in Table 6.

First of all, $^{57}\text{FeCl}_2$ with added $[\text{emim}]\text{Cl}$ ($\text{Fe}^{2+}/\text{Cl}^- = 1:7$) and water ($\text{Fe}^{2+}/\text{H}_2\text{O} = 1:18$) was dissolved in $[\text{emim}][\text{OTf}]$, and Mössbauer spectra were recorded. The spectrum obtained prior to nitrosylation could be deconvoluted into two overlapping quadrupole doublets with very similar isomer shifts of 1.02 and 1.05 mm/s. The shifts as well as the quadrupole splittings resemble the values found for high-spin tetrachloridoferrate(II) complexes described above. Both species are present in equal amounts as can be seen from the relative intensity values. The larger quadrupole splitting for the second compound can be explained, if we assume the formation of a chlorido-bridged diiron complex and thus with lower local symmetry around the metal center. The isomer shift (1.05 mm/s) is lower than the value found for iron(II) chloride dihydrate ($\text{FeCl}_2 \cdot 2\text{H}_2\text{O}$; 1.12 mm/s).^{47b} For this species a polymeric structure was determined such that each metal ion is surrounded by four in-plane chloride atoms with the two water molecules completing a distorted trans-octahedral arrangement. This could indicate that no water molecules coordinate to the iron center upon dissolving it in the IL. However, similar values were also obtained for “pure” tetrachloridoferrate(II) complexes ($[\text{C}_5\text{H}_7\text{S}_2]_2[\text{FeCl}_4]$, 1.15 mm/s; $[(\text{CH}_3)_4\text{N}]_2[\text{FeCl}_4]$, 1.25 mm/s; $[(\text{C}_2\text{H}_5)_4\text{N}]_2[\text{FeCl}_4]$, 1.16).⁶⁹

The product spectrum can be simulated by assuming the presence of two different species. The first one is presented by a doublet with parameters typical for the high-spin Fe(III) center (see Table 6), due to the presence of only weak ligands (like H_2O or Cl^-) in solution.^{47d,48a} The second component has a very high isomer shift (1.63 mm/s) and a quadrupole splitting close to zero. A compound with similar parameters was already observed in the nitrosylated IL solution without additionally added chloride ions (see Table 4). We suggested the presence

Table 6. Comparison of the Mössbauer Parameters for Species Obtained upon Dissolving $^{57}\text{FeCl}_2$ in $[\text{emim}][\text{OTf}]$ with Added Chloride and Varying Water Content before and after the Nitrosylation Reaction; The Proposed Iron Species Are Given for All Ascertained Values

	precursor, without NO			after saturation with NO		
IS	1.02	1.05		0.42	1.63	with extra H_2O
QS	2.24	2.91		1.48		
relative intensity, %	44	56		24	76	
possible species	$[\text{FeCl}_4]^{2-}$	$[\text{Fe}_2\text{Cl}_6]^{2-}$		Fe(III) , h.s.	Fe(II) , h.s.	
IS	1.02	1.05	0.66	0.41	1.31	extra dry IL
QS	2.31	2.93	0.63	1.46		
relative intensity, %	49	43	8	22	78	
possible species	$[\text{FeCl}_4]^{2-}$	$[\text{Fe}_2\text{Cl}_6]^{2-}$	Fe(III) impurity	Fe(III) , h.s.	Fe(II) , h.s.	

of a high-spin Fe(II) center with high local symmetry. A somewhat too high value of the isomer shift in the current spectrum could originate from a deficient fit. It is, however, remarkable that these species represent nearly 80% of the product mixture.

Furthermore, we performed Mössbauer measurements at the same high chloride content but in extra dried IL and without any added water; see Figure 13. The results are also presented

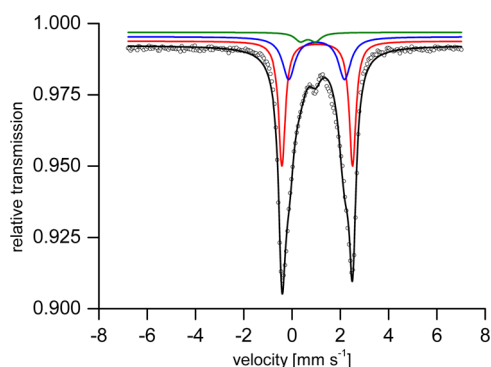


Figure 13. Zero-field Mössbauer spectra of $0.06 \text{ M } ^{57}\text{FeCl}_2$ in deoxygenated extra dried $[\text{emim}][\text{OTf}]$ (0.03 M water) with added $[\text{emim}]\text{Cl}$ ($\text{Fe}^{2+}/\text{Cl}^- = 1:7$) at 77 K (dots) fitted with three quadrupole doublets: (blue) $\text{IS} = 1.02 \text{ mm/s}$, $\text{QS} = 2.31 \text{ mm/s}$ —monomeric high-spin tetrachloridoferrate(II) complex; (red) $\text{IS} = 1.05 \text{ mm/s}$, $\text{QS} = 2.93 \text{ mm/s}$ —chloride-bridged diiron complex; (green) $\text{IS} = 0.66 \text{ mm/s}$, $\text{QS} = 0.63 \text{ mm/s}$ — Fe(III) impurities.

in Table 6 and show a clear similarity to those found in solution with a high water concentration. The spectrum of the frozen IL solution before nitrosylation reveals again two doublets, which can be ascribed to the high-spin mononuclear and chloride-bridged tetrachloridoferrate(II) species present in nearly equal amounts. The third component with the small isomer shift (0.66 mm/s) and quadrupole splitting (0.63 mm/s) indicates the presence of a small amount (8%) of a Fe(III) impurity in the studied solution.

The spectrum of the nitrosylated solution shows again the doublet of the high-spin (h.s.) Fe(III) center and a singlet of the h.s. Fe(II) species present in nearly the same ratio as in the solution with higher water content; see Figure 14. Thus, we conclude that, if there is any influence of the varying water content on the nature and/or composition of the species present in the IL solution, it is not detectable with the selected method.

On the basis of the Mössbauer results and the determined crystal structure, we conclude that a tetrachloridoferrate(II)

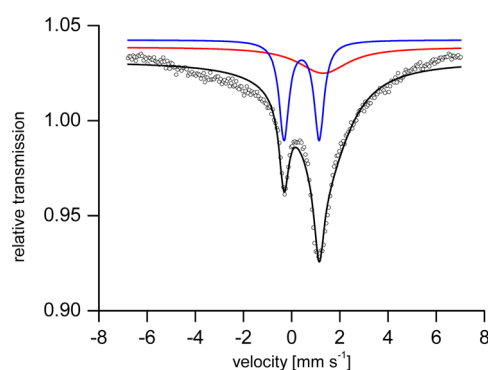
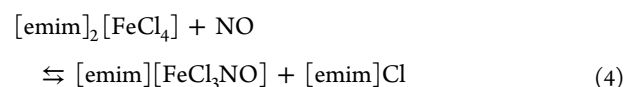


Figure 14. Zero-field Mössbauer spectrum of $0.06 \text{ M } ^{57}\text{FeCl}_2$ in deoxygenated extra dried $[\text{emim}][\text{OTf}]$ (0.03 M water) with added $[\text{emim}]\text{Cl}$ ($\text{Fe}^{2+}/\text{Cl}^- = 1:7$) after the reaction with NO at 77 K (dots) fitted with the quadrupole doublet, $\text{IS} = 0.41 \text{ mm/s}$, $\text{QS} = 1.46 \text{ mm/s}$ —h.s. Fe(III) species, and the singlet, $\text{IS} = 1.31 \text{ mm/s}$ —h.s. Fe(II) -nitrosyl product.

complex is formed in $[\text{emim}][\text{OTf}]$ solution with increased chloride content (added as $[\text{emim}]\text{Cl}$). The proposed reaction with NO can be expressed by the following equation:



The reversibility of the nitrosylation reaction was tested under these conditions and the equilibrium constant was determined thermodynamically, as described above. The estimated value is much higher than that found before in the IL solution without added $[\text{emim}]\text{Cl}$ (see Table 7), suggesting that more of the nitrosyl complex is formed under such conditions.

On the basis of the reported results, we suggest that the product species present in the Mössbauer spectrum as a singlet with a high isomer shift is the nitrosyl product generated in

Table 7. Equilibrium Constants for the Iron-Nitrosyl Complex Formation in Different Solvents

solvent	water ³³	$[\text{emim}][\text{OTf}]$	$[\text{emim}][\text{dca}]^{19}$
$K_{\text{eq}} [\text{M}^{-1}]$	1150 ± 50^a	420 ± 70^c	172 ± 20
	440 ± 110^b	1010 ± 300^d	

^aThermodynamically obtained value. ^bKinetically obtained value. ^c Cl^- anions in the solution originate mainly from the used iron(II) chloride. ^d Cl^- anions in the solution originate from the used iron(II) chloride and the added $[\text{emim}]\text{Cl}$.

[emim][OTf] as medium. First, this compound is present under all studied conditions, i.e., varying chloride and water concentrations; see Tables 4 and 6. Second, its fraction in the product mixture is linked to the equilibrium constant determined for the nitrosylation reaction under different conditions; see Table 8. In the solution with low chloride

Table 8. Comparison of the Equilibrium Constants Obtained for the Reaction with NO in [emim][OTf] as Medium with and without Added Chloride, and the Ratios of the Assumed Iron Nitrosyl Product in the Final Mixture According to Mössbauer Measurements

	low Cl ⁻ concentration	high Cl ⁻ concentration
K_{eq}	420 ± 70 M ⁻¹	1010 ± 300 M ⁻¹
ratio of the discussed iron species	28%	76%

concentration, viz. chloride originating only from the IL itself or from FeCl₂ used as source for Fe(II), the K_{eq} value is ~400 M⁻¹ and the content of the discussed iron species is ~30%. With increasing chloride content achieved by addition of [emim]Cl to FeCl₂ upon dissolution in [emim][OTf], the equilibrium constant is ~2.5 times larger as well as the content of the iron compound.

The Mössbauer experiments do not allow us a more explicit prediction about the structure of the discussed complex than that the iron center possesses high local symmetry. Furthermore, the parameters indicate that the metal center keeps the oxidation state of +2; thus, no oxidation to Fe(III) upon nitrosylation is observed, in contrast to the observations in [emim][dca]¹⁹ or water³³ as reaction medium. These results are in agreement with our EPR experiments, because a spin quartet state of $S = 3/2$ can also result from a Fe^{II}-NO[•] complex.

CONCLUSIONS

The goal of this study was to investigate the binding of NO to FeCl₂ in a noncoordinating IL [emim][OTf] as reaction medium. Because triflate is a weak donor ligand, the addition of water and/or chloride to the IL was required to increase the solubility of FeCl₂. Preliminary studies showed that the UV-vis product spectrum of the reversible binding of NO resembled the spectral characteristics obtained in water and [emim][dca] as solvents. A detailed analysis of the spectra, however, revealed that the {Fe-NO}⁷ species has Fe^{II}-NO[•] character in contrast to Fe^{III}-NO⁻ as found for the other solvents. Comparison of the formation constants obtained in [emim][OTf] and water, as well as the clear correlation between the water and chloride content of the ionic liquid and the solubility of the applied FeCl₂ salt, indicated that triflate is indeed a weak donor ligand and practically has no coordination ability in the studied system. Therefore, other potential ligands such as chloride and water are required to form the coordination sphere around the Fe(II) complex and to stabilize this complex in the IL medium.

On increasing the chloride concentration of the solution by addition of [emim]Cl, the composition of the reaction mixture shifted from complexes containing water and/or chloride ligands toward chloride-rich compounds. This process could be followed by Mössbauer spectroscopy, which indicated the presence of the tetrachloridoferrate complex in solution.

Furthermore, the structure of this species isolated directly from the ionic liquid was verified by X-ray crystallography.

The reaction mixture following nitrosylation was also examined by Mössbauer spectroscopy. The formed nitrosyl product is suggested to be [Fe^{II}Cl₃NO]⁻, which is present in the spectrum as a singlet with a high isomer shift and appears in the spectrum under all studied conditions. Its content in the reaction mixture is directly linked to the complex-formation constant. The obtained Mössbauer parameters indicate a high local symmetry around the iron center and suggest that upon NO binding no oxidation of Fe(II) to Fe(III) occurs, in contrast to the other solvents studied before. EPR and IR experiments support this proposal and reveal a spin quartet ground state ($S_{\text{e}} = 3/2$) and a less negative character of coordinated NO, respectively, compared to the other solvents studied before.

A comparison of our present results with reactions thoroughly studied in conventional solvents before indicates that the nature of the complex species present in ILs strongly depends on the applied solvent and/or additives used to modify the solubility properties of different ILs. Especially the donor property of the anionic component of the IL seems to play a decisive role when dealing with transition metal ions. It follows that, although different reactions can be successfully transferred from conventional solvents into ILs, the potential influence of this medium on the chemical behavior of the system has to be verified in advance by detailed spectroscopic and mechanistic investigations.

AUTHOR INFORMATION

Corresponding Author

*rudi.vaneldik@fau.de.

Notes

The authors declare no competing financial interest.

ACKNOWLEDGMENTS

The authors gratefully acknowledge continued financial support from the Deutsche Forschungsgemeinschaft. We thank Professor Axel Koenig and Philipp Keil from the Chair of Separation Science & Technology, University of Erlangen—Nürnberg, for performing the ion chromatographic analyses on [emim][OTf]. We also thank Dr. Marat Khusniyarov for assistance with the Mössbauer spectra and Dipl. Chem. Markus Walther for supporting us to solve some nasty problems while preparing the graphical material.

REFERENCES

- (1) (a) Marcus, Y. *Chem. Soc. Rev.* **1993**, *22*, 409–416. (b) Reichardt, C. *Solvents and Solvent Effects in Organic Chemistry*, 3rd ed.; Wiley-VCH: Weinheim, Germany, 2003. (c) Li, C. P.; Du, M. *Chem. Commun.* **2011**, *47*, 5958–5972. (d) Litwinienko, G.; Beckwith, A. L. J.; Ingold, K. U. *Chem. Soc. Rev.* **2011**, *40*, 2157–2163. (e) Subramanian, V. *Chem. React. Theory* **2009**, *379–393*. (f) Canuto, S.; Ribeiro, A. A. S. T.; de Alencastro, R. B. *Int. J. Quantum Chem.* **2011**, *111*, 1252–1255.
- (2) (a) Buncl, E.; Stairs, R. A.; Wilson, H. *The Role of the Solvent in Chemical Reactions*, 1st ed.; Oxford University Press: Oxford, U.K., 2003. (b) Truhlar, D. G. *Nat. Chem.* **2013**, *5*, 902–903. (c) Maltese, F.; van der Kooy, F.; Verpoorte, R. *Nat. Prod. Commun.* **2009**, *4*, 447–454. (d) Sato, H. *Understanding Chem. React.* **2003**, *24*, 61–99.
- (3) (a) Wypych, G., Ed. *Handbook of Solvents*; ChemTec Publishing: Toronto, 2001. (b) Dicks, A. P., Ed. *Green Organic Chemistry in Lecture and Laboratory*; CRC Press (Taylor & Francis Group): Boca Raton, FL, 2012.

- (4) (a) Knochel, P. *Modern Solvents in Organic Synthesis*; Springer, Berlin, 1999. (b) Adams, D. J.; Dyson, P. J.; Tavener, S. J. *Chemistry in Alternative Reaction Media*; Wiley, Chichester, U.K., 2004. (c) Kerton, F. M.; Marriott, R. *Alternative Solvents for Green Chemistry*, 2nd ed.; RCS Publishing: Cambridge, U.K., 2013. (d) Kerton, F. M.; Liu, Y.; Khaled, W.; Hawboldt, K. *Green Chem.* **2013**, *15*, 860–871. (e) MacMillan, D. S.; Murray, J.; Sneddon, H. F.; Jamieson, C.; Watson, A. J. B. *Green Chem.* **2012**, *14*, 3016–3019. (f) Breeden, S. W.; Clark, J. H.; Macquarrie, D. J.; Sherwood, J. *Green Solvents*. In *Green Techniques for Organic Synthesis and Medicinal Chemistry*; Zhang, W., Cue, B., Eds.; John Wiley & Sons: Chichester, U.K., 2012; Chapter 9, pp 243–257.
- (5) Kokorin, A., Ed. *Ionic Liquids: Applications and Perspectives*; InTech: Rijeka, Croatia, 2011.
- (6) Chiappe, C.; Pieraccini, D. *J. Phys. Org. Chem.* **2005**, *18*, 275–297.
- (7) (a) Anderson, J. L.; Ding, R.; Ellern, A.; Armstrong, D. W. *J. Am. Chem. Soc.* **2005**, *127*, 593–604. (b) Kosmulski, M.; Gustafsson, J.; Rosenholm, J. B. *Thermochim. Acta* **2004**, *412*, 47–53.
- (8) Smiglak, M.; Reichert, M. W.; Holbrey, J. D.; Wilkes, J. S.; Sun, L.; Thrasher, J. S.; Kirichenko, K.; Singh, S.; Katritzky, A. R.; Rogers, R. D. *Chem. Commun.* **2006**, *24*, 2554–2556.
- (9) (a) Earle, M. J.; Esperanca, J. M. S. S.; Gilea, M. A.; Lopes, J. N. C.; Rebelo, L. P. N.; Magee, J. W.; Seddon, K. R.; Widegren, J. A. *Nature* **2006**, *439*, 831–834. (b) Zaitsau, D. H.; Kabo, G. J.; Strechan, A. A.; Paulechka, Y. U.; Tschersch, A.; Verevkin, S. P.; Heintz, A. J. *Phys. Chem. A* **2006**, *110*, 7303–7306.
- (10) Neumann, J.; Steudte, S.; Cho, C.-W.; Thöming, J.; Stolte, S. *Green Chem.* **2014**, *16*, 2174–2184.
- (11) (a) Somers, A. E.; Khemchandani, B.; Howlett, P. C.; Sun, J.; MacFarlane, D. R.; Forsyth, M. *ACS Appl. Mater. Interfaces* **2013**, *5*, 11544–11553. (b) Escudero, L. B.; Castro, G. A.; Martinis, E. M.; Wuilloud, R. G. *Anal. Bioanal. Chem.* **2013**, *405*, 7597–7613. (c) Forte, A.; Bogel-Lukasik, E.; Bogel-Lukasik, R. *J. Chem. Eng. Data* **2011**, *56*, 2273–2279. (d) Trindade, C. A.; Visak, Z. P.; Bogel-Lukasik, R.; Bogel-Lukasik, E.; Nunes da Ponte, M. *Ind. Eng. Chem. Res.* **2010**, *49*, 4850–4857.
- (12) (a) Bansal, V.; Bhargava, S. K. *Ionic liquids as designer solvents for the synthesis of metal nanoparticles*. In *From Ionic Liquids: Theory, Properties, New Approaches*; Kokorin, A., Ed.; InTech: Rijeka, Croatia, 2011; pp 367–382. (b) Mudring, A.; Alammari, T.; Baecker, T.; Richter, K. *ACS Symp. Ser.* **2009**, *1030*, 177–188. (c) Morris, R. E. *Chem. Commun.* **2009**, *21*, 2990–2998. (d) Paczal, A.; Kotschy, A. *Monatsh. Chem.* **2007**, *138*, 1115–1123. (e) Haddleton, D. M.; Welton, T.; Carmichael, A. J. *Polymer synthesis in ionic liquids*. In *Ionic Liquids in Synthesis*, 2nd ed.; Wasserscheid, P., Welton, T., Eds.; Wiley-VCH Verlag: Weinheim, Germany, 2008; Chapter 2, pp 619–640.
- (13) (a) Li, H.; Bhadury, P. S.; Song, B.; Yang, S. *RSC Adv.* **2012**, *2*, 12525–12551. (b) Bica, K.; Leder, S.; Gaertner, P. *Curr. Org. Synth.* **2011**, *8*, 824–839. (c) Suarez, P. A. Z.; Ramalho, H. F. *Curr. Org. Chem.* **2013**, *17*, 229–237. (d) Fernandez-Alvaro, E.; Dominguez de Maria, P. *Curr. Org. Chem.* **2012**, *16*, 2492–2507.
- (14) (a) Huang, Y.; Yao, S.; Song, H. *J. Chromatogr. Sci.* **2013**, *51*, 739–752. (b) Meindersma, W.; De Haan, A. B. *Separation processes with ionic liquids*. In *Ionic Liquids UnCOILed*; Plechkova, N. V., Seddon, K. R., Eds.; Wiley: 2013; pp 119–179. (c) Graham, C. M.; Anderson, J. L. *Ionic liquids in separation science*. In *Ionic Liquids UnCOILed*; Plechkova, N. V., Seddon, K. R., Eds.; Wiley: 2013; pp 87–118. (d) Fontanals, N.; Borrull, F.; Marce, R. M. *Trends Anal. Chem.* **2012**, *41*, 15–26. (e) Wang, J.; Zheng, Y.; Zhang, S. *The application of ionic liquids in dissolution and separation of lignocellulose*. In *Clean Energy Systems and Experiences*; Eguchi, K., Ed.; InTech: Rijeka, Croatia, 2010; pp 71–84.
- (15) (a) Ferraz, R.; Branco, L. C.; Prudencio, C.; Noronha, J. P.; Petrovski, Z. *ChemMedChem* **2011**, *6*, 975–985. (b) Prechtel, M. H. G.; Sahler, S. *Curr. Org. Chem.* **2013**, *17*, 220–228. (c) Chaban, V. V.; Prezhdo, O. V. *J. Phys. Chem. Lett.* **2013**, *4*, 1423–1431. (d) Ahmed, E.; Breternitz, J.; Groh, M. F.; Ruck, M. *CrystEngComm* **2012**, *14*, 4874–4885. (e) Yuan, J.; Antonietti, M. *Polymer* **2011**, *52*, 1469–1482. (f) Torimoto, T.; Tsuda, T.; Okazaki, K.; Kuwabata, S. *Adv. Mater.* **2010**, *22*, 1196–221.
- (16) (a) Abbott, A. P.; Frisch, G.; Ryder, K. S. *Annu. Rev. Mater. Res.* **2013**, *43*, 335–358. (b) Hasanzadeh, M.; Shadjou, N.; Eskandani, M.; de la Guardia, M. *Trends Anal. Chem.* **2012**, *41*, 58–74. (c) Fujimoto, T.; Awaga, K. *Phys. Chem. Chem. Phys.* **2013**, *15*, 8983–9006.
- (17) (a) McNulty, J.; Cheekoori, S.; Bender, T.; Coggan, J. *Eur. J. Org. Chem.* **2007**, 1423–1428. (b) Daguinet, C.; Dyson, P. *Organometallics* **2006**, *25*, 5811–5816. (c) Vidis, A.; Laurenczy, G.; Küsters, E.; Sedelmeier, G.; Dyson, P. *J. Phys. Org. Chem.* **2007**, *20*, 109–114.
- (18) Begel, S.; Illner, P.; Kern, S.; Puchta, R.; van Eldik, R. *Inorg. Chem.* **2008**, *47*, 7121–7132.
- (19) Begel, S.; Heinemann, F. W.; Stopa, G.; Stochel, G.; van Eldik, R. *Inorg. Chem.* **2011**, *50*, 3946–3958.
- (20) Schmeisser, M.; van Eldik, R. *Inorg. Chem.* **2009**, *48*, 7466–7475.
- (21) Schmeisser, M.; van Eldik, R. *Dalton Trans.* **2014**, *43*, 15675–15692.
- (22) (a) Illner, P.; Begel, S.; Kern, S.; Puchta, R.; van Eldik, R. *Inorg. Chem.* **2009**, *48*, 588–597. (b) Kern, S.; Illner, P.; Begel, S.; van Eldik, R. *Eur. J. Inorg. Chem.* **2010**, *29*, 4658–4666.
- (23) Begel, S.; van Eldik, R. *Dalton Trans.* **2011**, *40*, 4892–4897.
- (24) Weckesser, D.; Jensen, D.; König, A. *GIT Labor-Fachz.* **2007**, 19–22.
- (25) Unpublished results; for the general procedure used to determine the solubility of NO, see ref 23.
- (26) Wasserscheid, P.; Welton, T. *Ionic liquids in synthesis*; Wiley-VCH: Weinheim, Germany, 2003; p 81.
- (27) (a) Spitzer, M.; Gartig, F.; van Eldik, R. *Rev. Sci. Instrum.* **1988**, *59*, 2092–2093. (b) Fleischmann, K. F.; Conze, G. E.; Stranks, R. D.; Kelm, H. *Rev. Sci. Instrum.* **1974**, *45*, 1427–1430.
- (28) Nova Werke AG, CH-8307 Effretikon, Vogelsangstrasse.
- (29) SADABS 2.06; Bruker AXS, Inc.: Madison, WI, 2009.
- (30) SHELXTL NT 6.12; Bruker AXS, Inc.: Madison, WI, 2002.
- (31) (a) Franke, A.; Roncaroli, F.; van Eldik, R. *Eur. J. Inorg. Chem.* **2007**, *6*, 773–798. (b) Franke, A.; van Eldik, R. *Eur. J. Inorg. Chem.* **2013**, *4*, 460–480. (c) NOx Related Chemistry. In *Advances in Inorganic Chemistry*; Olabe, J., van Eldik, R., Eds.; Elsevier Academic Press: San Diego, 2015; Vol. 67.
- (32) (a) Schnepfenseper, T.; Finkler, S.; Czup, A.; van Eldik, R.; Heus, M.; Nieuwenhuizen, P.; Wreesmann, C.; Abma, W. *Eur. J. Inorg. Chem.* **2001**, *2*, 491–501. (b) Schnepfenseper, T.; Wanat, A.; Stochel, G.; Goldstein, S.; Meyerstein, D.; van Eldik, R. *Eur. J. Inorg. Chem.* **2001**, *9*, 2317–2325. (c) Schnepfenseper, T.; Wanat, A.; Stochel, G.; van Eldik, R. *Inorg. Chem.* **2002**, *41*, 2565–73.
- (33) Wanat, A.; Schnepfenseper, T.; Stochel, G.; van Eldik, R.; Bill, E.; Wieghardt, K. *Inorg. Chem.* **2002**, *41*, 4–10.
- (34) (a) Das, S.; Bhar, K.; Fun, H.-K.; Chantrapomma, S.; Ghosh, B. *K. Inorg. Chim. Acta* **2010**, *363*, 784–792. (b) Sarkar, B. N.; Bhar, K.; Chattopadhyay, S.; Das, S.; Mitra, P.; Ghosh, B. K. *J. Mol. Struct.* **2010**, *963*, 35–40. (c) Ma, K.; Shi, Q.; Hu, M.; Cai, X.; Huang, S. *Inorg. Chim. Acta* **2009**, *362*, 4926–4930. (d) Mautner, F. A.; Mikuriya, M.; Ishida, H.; Sakiyama, H.; Louka, F. R.; Humphrey, J. W.; Massoud, S. *Inorg. Chim. Acta* **2009**, *362*, 4073–4080. (e) Das, A.; Marschner, C.; Cano, J.; Baumgartner, J.; Ribas, J.; El Fallah, M. S.; Mitra, S. *Polyhedron* **2009**, *28*, 2436–2442. (f) Liu, H.; Tian, J.-L.; Kou, Y.-Y.; Gu, W.; Feng, L.; Yan, S.-P.; Liao, D.-Z. *Anorg. Allg. Chem.* **2008**, *634*, 1565–1569.
- (35) Kohout, J.; Jager, L.; Hvastijova, M.; Kozisek, J. *J. Coord. Chem.* **2000**, *51*, 169–218.
- (36) Berto, T. C.; Speelman, A. L.; Zheng, S.; Lehnert, N. *Coord. Chem. Rev.* **2013**, *257*, 244–259.
- (37) Radoń, M.; Broclawik, E.; Pierloot, K. *J. Chem. Phys. B* **2010**, *114*, 1518–1528.
- (38) (a) Chiou, Y.-M.; Que, L., Jr. *Inorg. Chem.* **1995**, *34*, 3270–3278. (b) Li, J.; Banerjee, P. L.; Brennessel, W. W.; Chavez, F. A. *Inorg. Chem.* **2014**, *53*, 5414–5416.

- (39) (a) Kurtikyan, T. S.; Ford, P. C. *Coord. Chem. Rev.* **2008**, *252*, 1486–1496. (b) Machura, B. *Coord. Chem. Rev.* **2005**, *249*, 2277–2307. (c) Mingos, D. M. P.; Sherman, D. J. *Adv. Inorg. Chem.* **1989**, *34*, 293. (d) McCleverty, J. A. *Chem. Rev.* **1979**, *79*, 53.
- (40) Feelisch, M., Stamler, J., Eds. *Methods in Nitric Oxide Research*; John Wiley & Sons Ltd.: West Sussex, U.K., 1996; Chapter 29.
- (41) Schmeisser, M.; Illner, P.; Puchta, R.; Zahl, A.; van Eldik, R. *Chem.—Eur. J.* **2012**, *18*, 10969–10982.
- (42) Brookes, J. F.; Slenkamp, K. M.; Lynch, M. S.; Khalil, M. J. *Phys. Chem. A* **2013**, *117*, 6234–6243.
- (43) Mayer, U.; Gutmann, V.; Gerger, W. *Monatsh. Chem.* **1975**, *106*, 1235–1257.
- (44) (a) Brown, C. A.; Pavlosky, M. A.; Westre, T. E.; Zhang, Y.; Hedman, B.; Hodgson, K. O.; Solomon, E. I. *J. Am. Chem. Soc.* **1995**, *117*, 715–732. (b) Westre, T. E.; Di Cicco, A.; Filippini, A.; Natoli, C. R.; Hedman, B.; Solomon, E. I.; Hodgson, K. O. *J. Am. Chem. Soc.* **1994**, *116*, 6757–6768.
- (45) Hauser, C.; Glaser, T.; Bill, E.; Weyhermüller, T.; Wieghardt, K. *J. Am. Chem. Soc.* **2000**, *122*, 4352–4365.
- (46) (a) Carver, G.; Dobe, C.; Jensen, T. B.; Tregenna-Piggott, P. L. W.; Janssen, S.; Bill, E.; McIntyre, G. J.; Barra, A.-L. *Inorg. Chem.* **2006**, *45*, 4695–4705. (b) Greenwood, N. N.; Gibb, T. C. *Mössbauer Spectroscopy*; Chapman and Hall Ltd.: London, 1971.
- (47) (a) Nunes, G. G.; Bottini, R. C. R.; Reis, D. M.; Camargo, P. H. C.; Evans, D. J.; Hitchcock, P. B.; Leigh, G. J.; Sá, E. L.; Soares, J. F. *Inorg. Chim. Acta* **2004**, *357*, 1219–1228. (b) Burbridge, C. D.; Goodgame, D. M. L. *J. Chem. Soc. A* **1968**, 1410–1413. (c) Reisner, E.; Telser, J.; Lippard, S. J. *Inorg. Chem.* **2007**, *46*, 10754–10770. (d) Zhao, M.; Helms, B.; Slonkina, E.; Friedle, S.; Lee, D.; DuBois, J. B.; Hedman, K. O.; Hodgson, J.; Frechet, M. J.; Lippard, S. J. *J. Am. Chem. Soc.* **2008**, *130*, 4352–4363.
- (48) (a) Ginsberg, A. P.; Robim, M. B. *Inorg. Chem.* **1963**, *2*, 817–822. (b) Feist, M.; Kunze, R.; Neubert, D.; Witke, K.; Mehner, H.; Kemnitz, E. *Thermochim. Acta* **2000**, *361*, 53–60.
- (49) Riedel, E.; Prick, D.; Pfitzner, A.; Lutz, H. D. *Z. Anorg. Allg. Chem.* **1993**, *619*, 901–904.
- (50) Wile, B. M.; Trovitch, R. J.; Bart, S. C.; Tondreau, A. M.; Lobkovsky, E.; Milsman, C.; Bill, E.; Wieghardt, K.; Chirik, P. J. *Inorg. Chem.* **2009**, *48*, 4190–4200.
- (51) Lauher, J. W.; Ibers, J. A. *Inorg. Chem.* **1975**, *14*, 348–352.
- (52) (a) Cotton, F. A.; Murillo, C. A. *Inorg. Chem.* **1975**, *14*, 2467–2469. (b) Kistenmacher, T. J.; Stucky, G. D. *Inorg. Chem.* **1968**, *7*, 2150. (c) Wyrzykowski, D.; Maniecki, T.; Pattek-Janczyk, A.; Stanek, J.; Warnke, Z. *Thermochim. Acta* **2005**, *435*, 92–98.
- (53) Hitchcock, P. B.; Seddon, K. R.; Welton, T. *J. Chem. Soc., Dalton Trans.* **1993**, 2639–2643.
- (54) (a) Hayashi, S.; Saha, S.; Hamaguchi, H. *IEEE Trans. Magn.* **2006**, *42*, 12–14. (b) De Pedro, I.; Rojas, D. P.; Albo, J.; Luis, P.; Irabien, A.; Blanco, J. A.; Fernandez, J. R. *J. Phys.: Condens. Matter* **2010**, *22*, 296006:1–296006:4. (c) Herber, R. H.; Nowik, I.; Kostner, M. E.; Kahlenberg, V.; Kreutz, C.; Laus, G.; Schottenberger, H. *Int. J. Mol. Sci.* **2011**, *12*, 6397–6406 and literature cited there.
- (55) Sitze, M. S.; Schreiter, E. R.; Patterson, E. V.; Freeman, R. G. *Inorg. Chem.* **2001**, *40*, 2298–2304.
- (56) (a) Hurley, F. H.; Wier, T. P. *J. Electrochem. Soc.* **1951**, *98*, 203–206. (b) Hurley, F. H.; Wier, T. P. *J. Electrochem. Soc.* **1951**, *98*, 207–212. (c) Hurley, F. H. Electrodeposition of Aluminum. U.S. Pat. 4,446,331, 1948. (c1) Wier, T. P., Jr. U.S. Pat. 4,446,350, 1948. (c2) Wier, T. P., Jr.; Hurley, F. H. U.S. Pat. 4,446,349, 1948. (d) Chum, H. L.; Koch, V. R.; Miller, L. L.; Osteryoung, R. A. *J. Am. Chem. Soc.* **1975**, *97*, 3264–3265.
- (57) Hussey, C. L. *Pure Appl. Chem.* **1988**, *60*, 1763–1772.
- (58) (a) Carlin, R. T.; Osteryoung, R. A. *Inorg. Chem.* **1988**, *27*, 1482–1488. (b) Barnard, P. A.; Sun, I.-W.; Hussey, C. L. *Inorg. Chem.* **1990**, *29*, 3670–3674.
- (59) Carlin, R. T.; Osteryoung, R. A.; Wilkes, J. S.; Rovang, J. *Inorg. Chem.* **1990**, *29*, 3003–3009.
- (60) Laher, T. M.; Hussey, C. L. *Inorg. Chem.* **1983**, *22*, 3247–3251.
- (61) Laher, T. M.; Hussey, C. L. *Inorg. Chem.* **1982**, *21*, 4079–4083.
- (62) (a) Lawrance, G. A. *Chem. Rev.* **1986**, *86*, 17–33. (b) Babai, A.; Mudring, A.-V. *Inorg. Chem.* **2006**, *45*, 3249. (c) Hayashida, T.; Kondo, H.; Terasawa, J.; Kirchner, K.; Sunada, Y.; Nagashima, H. *J. Organomet. Chem.* **2007**, *692*, 382–394.
- (63) Wolf, S.; Lan, Y.; Powell, A.; Feldmann, C. *Z. Naturforsch.* **2013**, *68b*, 3–9.
- (64) Genre, C.; Jeanneau, E.; Bousseksou, A.; Luneau, D.; Borshch, S. A.; Matouzenko, G. S. *Chem.—Eur. J.* **2008**, *14*, 697–705.
- (65) Taylor, R.; Kennard, O. *J. Am. Chem. Soc.* **1982**, *104*, 5063.
- (66) Wang, F.; Wu, X.-Y.; Zhao, Z.-G.; Zhang, Q.-S.; Xie, Y.-M.; Yu, R.; Lu, C.-Z. *Inorg. Chim. Acta* **2010**, *363*, 1320–1324 and literature cited therein.
- (67) Abdul-Sada, A. K.; Al Juaid, S.; Greenway, A. M.; Hitchcock, P. B.; Howells, M. J.; Seddon, K. R.; Welton, T. *Struct. Chem.* **1990**, *1*, 391.
- (68) (a) Gibb, T. C.; Greenwood, N. N. *J. Chem. Soc.* **1965**, 6989–6991. (b) Styczeń, E.; Pattek-Janczyk, A.; Gazda, M.; Józwiak, W. K.; Wyrzykowski, D.; Warnke, Z. *Thermochim. Acta* **2008**, *480*, 30–34. (c) Leech, D. H.; Machin, D. J. *J. Inorg. Nucl. Chem.* **1975**, *37*, 2279–2282.
- (69) Mathur, H. B.; Gupta, M. P. *Chem. Phys. Lett.* **1969**, *3*, 191–194.